Spectrochimica Acta Part A: Molecular and Biomolecular Spectroscopy 150 (2015) 94–103

Contents lists available at ScienceDirect

Spectrochimica Acta Part A: Molecular and Biomolecular Spectroscopy

journal homepage: www.elsevier.com/locate/saa

Thiophene aldehyde-diamino uracil Schiff base: A novel fluorescent probe for detection and quantification of cupric, silver and ferric ions

Hassan H. Hammud [a,b,*], Shawky El Shazly [b], Ghassan Sonji [b], Nada Sonji [b], Kamal H. Bouhadir [c,*]

[a] Department of Chemistry, Faculty of Science, King Faisal University, Al-Ahsa 31982, Saudi Arabia
[b] Department of Chemistry, Faculty of Science, Beirut Arab University, Debbieh, Lebanon
[c] Department of Chemistry, Faculty of Arts and Sciences, American University of Beirut, Beirut, Lebanon

HIGHLIGHTS

- A novel Schiff base fluorescent chemosensor was easily prepared by a one-step reaction.
- The probe shows significant fluorescence quenching in presence of Ag^+, Cu^{2+} and Fe^{3+} ions.
- Limits of detection can reach 0.132 μM (Ag^+), 0.088 μM (Cu^{2+}) and 0.037 μM (Fe^{3+}).
- The analytical method was validated for the assay of the three cations in real samples.

GRAPHICAL ABSTRACT

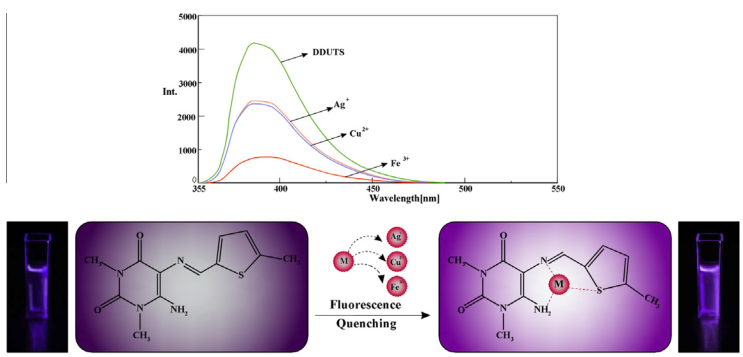

ARTICLE INFO

Article history:
Received 17 January 2015
Received in revised form 4 April 2015
Accepted 7 May 2015
Available online 20 May 2015

Keywords:
5,6-Diamino-1,3-dimethyluracil
Methyl-2-thiophenecarboxaldehyde
Schiff base
Fluorescence probe
$Ag^+/Cu^{2+}/Fe^{3+}$ ions
Water pollution

ABSTRACT

A new Schiff base from the condensation of 5,6-diamino-1,3-dimethyluracil with 5-methylthiophene-2-carboxaldehyde was synthesized. The compound was characterized by spectral data (UV–Vis, IR, ^{1}H NMR, fluorescence, MS). Ethanolic solutions of the Schiff base exhibit a strong fluorescence emission at 385 nm (λ_{ex} = 341 nm), and have been employed as a "turn-off" fluorescent probe for selective detection of Ag^+, Cu^{2+} and Fe^{3+} ions in presence of other cations such as Na^+, K^+, Ca^{2+} and Mg^{2+} ions abundant in natural water. The interaction between the tested compound and copper, silver or iron ions is associated with a significant fluorescence decrease, showing detection limits of 2.1–14.2 ppb. Under optimal conditions, the developed sensor was successfully employed to determine Ag^+, Cu^{2+} and Fe^{3+} ions in real samples and proved to be selective and sensitive.

Introduction

Heavy metals are widely spread in the environment. Humans are exposed to them through various pathways, such as food, mining, industrial productions, untreated sewage sludge, combustion by-products and atmospheric emissions [1]. Heavy metal contamination has become an increasingly serious threat to human health and ecology. Due to their toxicity, there is an obvious need to their detection and determination at trace levels [2].

The essentiality of iron and copper is based on their role as metalloenzymes. These metals are cofactors of large number of enzymes. However, a high supplementary iron causes pathological events such as the iron oxides deposition in Parkinson's disease, cirrhosis, liver cancer, cardiac arrhythmias and diabetes. Copper surplus had been associated with liver damage, jaundice, kidney failure, hemolysis, neurodegenerative diseases and hemoglobinuria [3,4].

* Corresponding authors at: Department of Chemistry, Faculty of Science, King Faisal University, Al-Ahsa 31982, Saudi Arabia (H.H. Hammud).

E-mail addresses: hhammoud@kfu.edu.sa (H.H. Hammud), kb05@aub.edu.lb (K.H. Bouhadir).

http://dx.doi.org/10.1016/j.saa.2015.05.038
1386-1425/

Silver occurs naturally in elemental form in various ores. In industry, silver is used in the manufacture of silver nitrate, silver bromide and other photographic chemicals, water distillation equipment, mirrors, silver plating equipment, special batteries, table cutlery, jewelry, dental medical and scientific equipment including amalgams and application in the fields of material science, chemistry and physics. In some countries silver oxide is used to disinfect water supplies, causing occasional raise in tap water silver levels. The importance of nano-silver (nAg) is due to its antimicrobial properties. Silver nanoparticles (Ag-np) have gained much popularity recently owing to the broad spectrum of antimicrobial activity. However, with the large consumption of manufactured nanomaterials and nanoparticles, silver may enter the aquatic ecosystems, posing serious possible risks to the environment. Ashen gray discoloration of the skin and other body tissues are the most important symptoms of silver poisoning [5,6]. Accordingly, enforceable standards or "MCLs" were established by the U.S. Environmental Protection Agency (EPA) in order to protect the public against consumption of drinking water contaminants that present a risk to human health, where "MCL" is the maximum allowable amount of a contaminant in drinking water which is delivered to the consumer. The MCLs for silver, copper and iron in drinking water are 0.05 ppm (0.46 μM), 1.0 ppm (15.7 μM) and 0.3 ppm (5.37 μM), respectively [7]. Therefore, the identification and measurement of Ag^{+}, Cu^{2+} and Fe^{3+} ions in samples have become increasingly important.

Various approaches are described in the literature for the detailed analysis of heavy metals in environmental, biological and food samples. These include atomic absorption spectroscopy, inductively coupled plasma optical emission spectrometry and inductively coupled plasma mass spectrometry (ICPMS), atomic fluorescence spectrometry (AFS), X-ray fluorescence (XRF) and electrochemical methods. The drawbacks is the requirement of sophisticated instrumentation and skilled personnel, and there is, therefore, a need for simpler methods. Fluorescence spectroscopy is a powerful analytical technique for determination of heavy metal ions owing to its simplicity, high sensitivity and widespread availability of equipment for analysis [8]. Recently, several groups have reported the determination of silver, copper and iron ions using fluorescent probes. Silver ions have been fluorometrically detected by novel benzimidazole-based spirobifluorene derivative [9], SYBR Green I and a silver(I)-specific cytosine-rich oligonucleotide [10], coumarin dithioate derivative [11], naphthalimide and thiosemicarbazide-based sensor [12], graphene-based sensor [13], aza-crown-ether-appended xanthene [14], twin-cyano-sti lbene [15] and by the condensation product of acetylferrocene and ethylenediamine [16].

Copper ion fluorescent sensors include heptamethine cyanine-based near-infrared fluorescent probe [17], dansyl-based probe [18], 6-(*N*,*N*-dimethylamino)-2-naphthoylacryl acid [19], triarylpyrazoline-based Cu(I) sensor [20], coumarin Schiff base [21], near-infrared fluorescent probe based on photo-induced electron transfer mechanism [22], bis-benzimidazolyldiamide-based probe [23], riboflavin-stabilized gold nanoclusters [24], [3-diam inophenazine, 1,2-diamino-anthraquinone and 2,4-dinitrophen ylhydrazine] [25], coumarin-based sensor [26,27], dehydroabietyl derivative bearing a 2-(2′-hydroxyphenyl) benzimidazole unit [28], rhodamine B hydrazide hydrazone derivative [29], carboxylic acid-functionalized tris(2,2′-bipyridine)-ruthenium(II) complex [30], thiourea-based probe [31], carbazole-based Schiff base [32], rhodamine-based probe [33], silver nanoclusters (Ag NCs) [34], 1,8-diaminonaphthalene-based sensor [35] and malonamide fluoroionophore [36].

Ferric ion fluorescent sensors include carbogenic nanoparticles (NPs) [37], naphthalimide-based probe [38], Europium metal with chelating terpyridine sites [39], pyoverdin [40], FITC/Au_1Ag_4@SiO_2 nanoparticles [41], 2-(-4-aminophenyl)-benzothiazole and 2-picolylamine derivatives [42], *N*-phenyl-2-(2-hydroxynap hthale n-1-ylmethylene)hydrazinecarbothioamide [43], coumarin or fluorescein and 3-hydroxy-pyridin-4-one or 3-hydroxy-pyran-4-one [44], perylenetetracarboxylicdiimide [45], calcein [46], coumarin-based probe [26], rhodamine-based sensor [47] and deprotection of acetal reaction [48].

In recent years, metal ion sensors have attracted considerable attention due to their applications in clinical toxicology, environmental bioinorganic chemistry, bioremediation and waste management. It is of great importance designing a sensor, where the fluorescence of the receptor molecule changes in presence of analyte. Fluorescent probes offer several advantages over conventional methods of water analysis, such as continuous online monitoring and no need for reagents or sample preparation, high sensitivity, non-destructive, small sample size, rapidity and simplicity [49–51]. Encouraged by these considerations, we developed DDUTS as a novel fluorescence probe for Ag^{+}, Cu^{2+} and Fe^{3+} ions in aqueous solutions. Reports on fluorescent sensors for more than one metal ions are rare and is known for a few combination of metal ions, like Cu^{2+}, Ni^{2+} [52]; Zn^{2+}, Ni^{2+} [53,54]; Cu^{2+}, Zn^{2+} [55]; Cu^{2+}, Hg^{2+} [31]; Cu^{2+}, Fe^{3+} [26]; Mg^{2+}, Zn^{2+} [56]; Ag^{+}, Zn^{2+} [16]; Ni^{2+}, Fe^{3+} [45]; Hg^{2+}, Ag^{+} [11,57]; F^{-}, Cu^{2+} [58]; Pb^{2+}, K^{+} [59] and Pb^{2+}, Al^{3+} [60]. To the best of our knowledge, fluorescence sensing for ternary cation samples is still lacking in the literature, which shows the importance of the developed fluorescent sensor in both detection and quantification of Ag^{+}, Cu^{2+} and Fe^{3+} ions. The present chemosensor can be easily prepared. Thus it has application advantage over complicated or time-consuming synthesis.

Experimental

Chemicals and reagents

All the materials for the synthesis were of the highest commercial quality and used without further purification. All the solvents used were of analytical reagent grade. Water was double distilled. The solutions of the metal ions were prepared from their chloride or nitrate salts.

Equipments

The progress of reaction was monitored by TLC using silica gel plates 60 F254. The melting point was measured with a

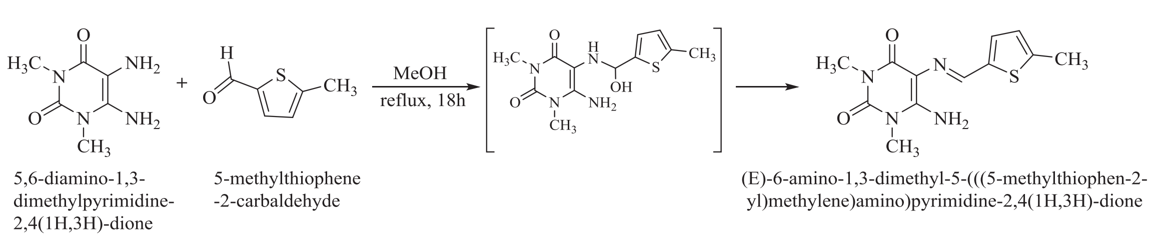

Scheme 1. Synthetic pathway of 6-amino-1,3-dimethyl-6-(((5-methylthiophen-2-yl)methylene)amino)pyrimidine-2,4(1H,3H)-dione.

Gallenkamp apparatus. IR spectrum was recorded in KBr pellet, on a Nicolet iS 10 FT/IR spectrophotometer. ^{1}H NMR spectra were recorded on a Bruker 500 MHz NMR spectrometer in $CDCl_3$ using tetramethylsilane (TMS) as the internal standard; chemical shifts are reported in ppm, and signals are expressed as s (singlets), d (doublets) and m (multiplets). Mass spectra were obtained in Agilent 1100-Bruker Esquire HCT liquid chromatograph-mass spectrometer (Kamal A. Shair Central Research Science Laboratory (KAS CRSL) – AUB). The spectrofluorometric measurements were carried out at room temperature on a Jasco FP-8300 spectrofluorometer (Instrumental Analytical Laboratory – BAU).

Synthesis and characterization of the Schiff base (6-amino-1,3-dimethyl-6-(((5-methylthiophen-2-yl)methylene)amino)pyrimidine-2,4(1H,3H)-dione) [DDUTS]

Methyl-2-thiophenecarboxaldehyde (2.45 mL, 23 mmol) was added drop-wise to a solution of 5,6-diamino-1,3-dimethyluracil hydrate (2.16 g, 11.5 mmol) in 150 mL methanol. The mixture was heated under reflux for 30 min, followed by the addition of a solution of 0.1 g p-toluenesulfonic acid in 5 mL methanol. The reflux was continued for 18 h. The hot mixture was poured over crushed ice and the solid was collected, recrystallized from hot ethanol and dried under reduced pressure to yield 1.62 g of orange solid (50% yield), m.p. 236–238 °C.

^{1}H NMR (300 MHz, $CDCl_3$) 2.49 (s, 3H, CH_3-thiophene), 3.37 (s, 3H, CH_3-uracil), 3.5 (s, 3H, CH_3-uracil), 5.64 (s, 2H, NH_2), 6.71–6.72 (d, 1H, Ar-CH-thiophene), 7.09–7.1 (d, 1H, Ar-CH-thiophene), 9.77 (s, 1H, CH=N). FT-IR (KBr, cm^{-1}) 3297, 3411 (N—H), 1691 (C=O), 1657 (C=C), 1597 (C=N), 680 (C—S). MS (EI): m/z (%) = 278.7 (100) [M^+].

Preparation of metal ions standard solutions

The nitrate and chloride salts of the metal were dissolved in double distilled water to prepare 2.0 mg/mL stock solutions. The stock solutions were further diluted with the same solvent to 0.20 mg/mL.

As most of tested metal ions are highly toxic and have adverse effects on human health, all experiments involving heavy metal ions and other toxic chemicals should be performed with protective gloves. The waste solutions containing heavy metal ions should be collectively reclaimed to avoid polluting the environment.

Fluorescence titration of DDUTS with different metal ions

A solution of 0.14 μM DDUTS was prepared in ethanol. Titration experiments were carried out in 1 cm quartz cuvette at room temperature. 2 mL of DDUTS solution was placed in the quartz cell and the florescence spectrum was recorded, it was then titrated by successive additions, in small portions (10 μL), of the solution of corresponding metal salt (0.020 mg/mL in water) and fluorescence intensity changes (λ_{ex} = 341 nm, λ_{em} = 385 nm) were recorded at room temperature each time.

Results and discussion

A new uracil/thiophene-based fluorescent sensor is described in scheme 1 that exhibits fluorescence quenching in the presence of Ag^+, Cu^{2+} and Fe^{3+} ions, with high selectivity over other metal cations. Monitoring of heavy metal ions in aquatic ecosystems is always an important issue because these ions may be present in sub-micromolar range and can exert adverse effects on the environment and also on human health. One of the most commonly used types of chemosensors is the fluorescent-based type. The success of this group of sensors may be explained by the several advantages that distinguish fluorescence from all other methods used in chemical sensing. Firstly, its ultra-high sensitivity, which is particularly required whenever the analyte to be studied is present in trace amounts. High response time is the second important feature of fluorescence, which can be as fast as 10^{-8}–10^{-10} s.

Schiff bases have been very important in the development of coordination chemistry, in part due to their capability to form stable complexes with the majority of the transition metals. The ability to stabilize most metals in different oxidation states also enhances their performance in catalytic processes. In the field of bioinorganic chemistry, Schiff base complexes have received careful attention, due to their role in providing synthetic models for the metal-containing sites in metallo-proteins and enzymes. Regarding their applications in chemical sensing, more specifically in

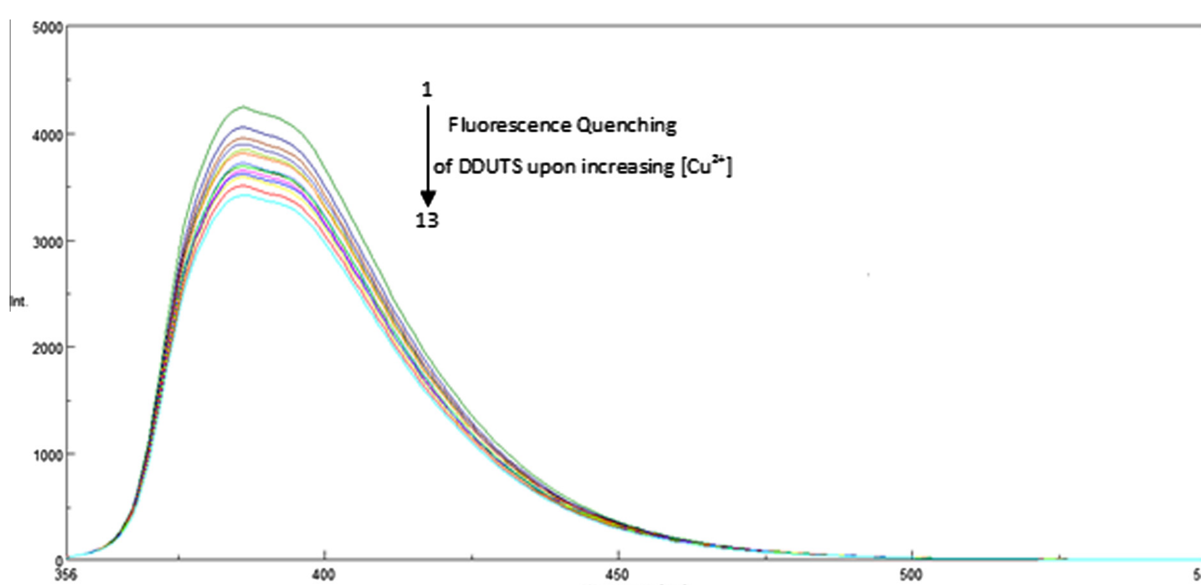

Fig. 1. Fluorescence quenching of DDUTS (0.14 μM in ethanol) upon exposure to different concentrations of cupric ion, from top to bottom, (0, 11.6, 23, 34.2, 45.1, 55.8, 86.9, 126, 144, 162, 196, 227, 242 μM). λ_{ex} = 341 nm, λ_{em} = 385 nm.

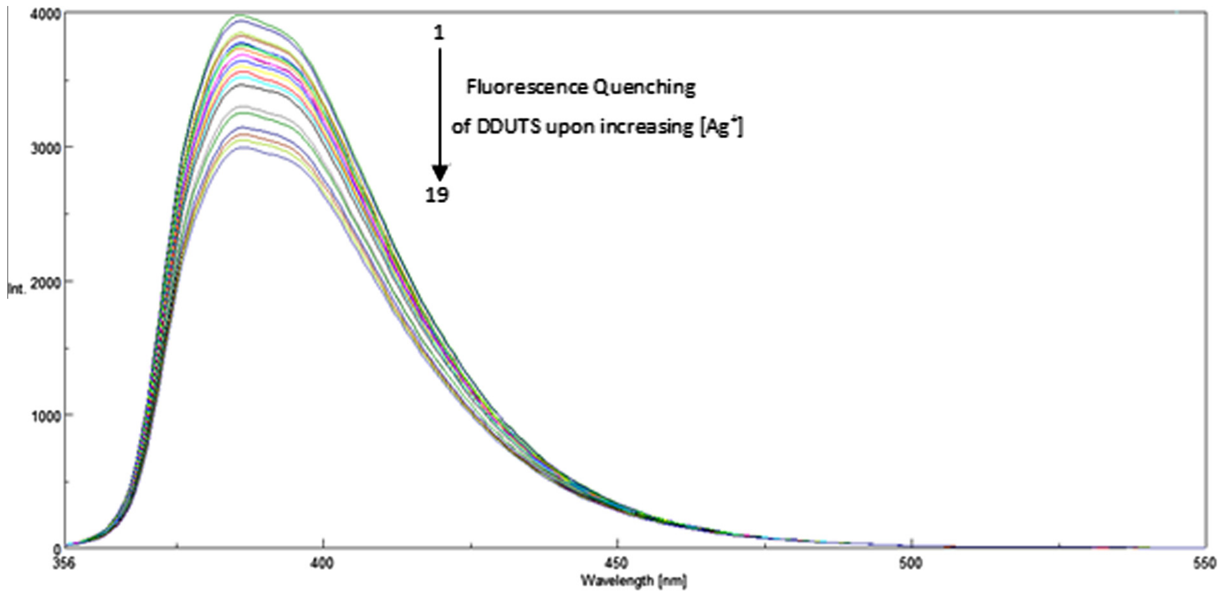

Fig. 2. Fluorescence quenching of DDUTS (0.14 μM in ethanol) upon exposure to different concentrations of silver ion, from top to bottom, (0, 23.1, 45.3, 66.6, 87.2, 107, 126.1, 144.6, 162.4, 179.6, 196.2, 212.3, 227.9, 257.6, 271.7, 298.7, 311.7, 324.2, 336.4 μM). λ_{ex} = 341 nm, λ_{em} = 385 nm.

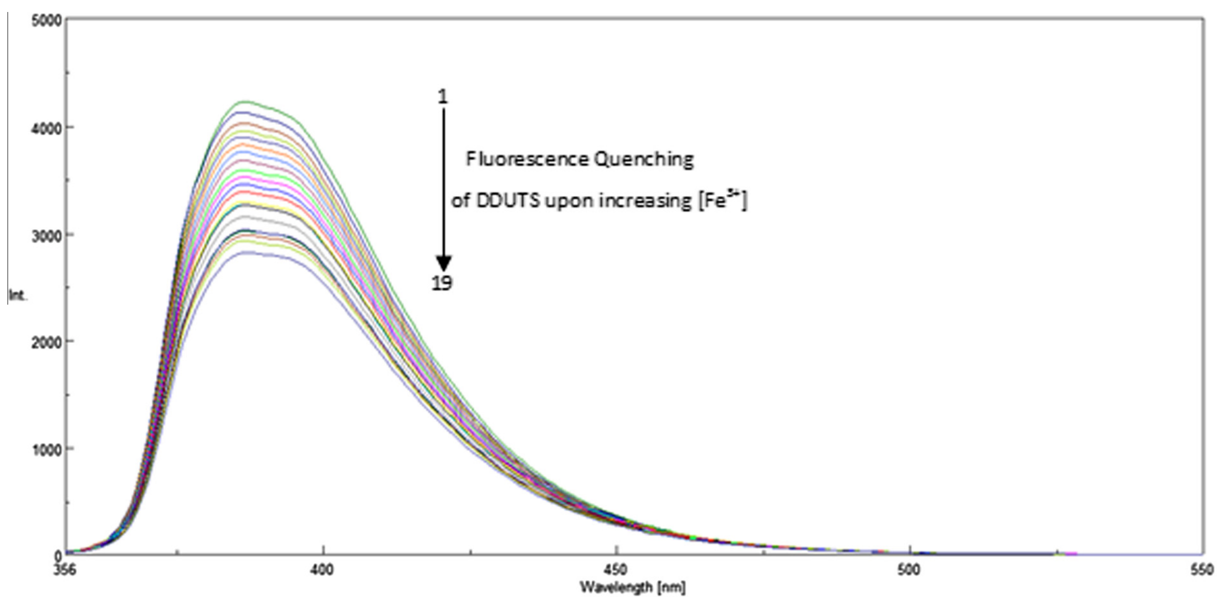

Fig. 3. Fluorescence quenching of DDUTS (0.14 μM in ethanol) upon exposure to different concentrations of ferric ion, from top to bottom, (0, 14.5, 28.5, 41.9, 54.8, 67.3, 79.3, 90.9, 102.1, 123.3, 143.2, 152.7, 161.9, 170.8, 179.4, 187.7, 195.9, 203.7, 211.4 μM). λ_{ex} = 341 nm, λ_{em} = 385 nm.

detection of cations, Schiff bases offer the advantage of possessing a good electron-donating group, the nitrogen atom with its lone electron pair can easily coordinate metal ions. Upon coordination, the properties of the system can be modulated, accordingly to the type of cation and its oxidation state.

The probe (DDUTS) was conveniently synthesized by the nucleophilic addition of 5,6-diamino-1,3-dimethyluracil to 5-methy l-2-thiophenecarboxaldheyde via the carbinolamine intermediate which underwent dehydration to form the corresponding imine (scheme 1). The structure of the Schiff base was elucidated on the basis of NMR, FTIR and MS analysis. The FTIR spectrum of the molecule showed the appearance of the NH-stretching vibrations at 3297 and 3411 cm^{-1}. The strong bands observed at 1691 and 1657 cm^{-1} correspond to C=O and C=C stretching vibrations, respectively. The bands at 1597 and 680 cm^{-1} indicated the presence of C=N and C—S bonds, respectively. Further characterization by ^{1}H NMR and mass spectrometry confirmed the structure of the compound. The singlet appearing at 9.77 ppm is assigned for the CH=N proton. Thiophene aromatic protons appeared as two doublets at 6.71 and 7.09 ppm; the resonance of the three methyl-groups protons appear as singlets at 2.49 ppm (thiophene) and 3.37, 3.5 ppm (uracil). The singlet appearing at 5.64 ppm is assigned for the NH_2 group protons.

Literature survey reveals that Schiff base chemosensors have been prepared in mixed aqueous media for detection of different cations and anions, this includes the application of: salicylimine-based chemosensor solution in 10% bistris/THF buffer (0.01 M, pH 7.0) for detection of cyanide ion [61]; napthalimide-based probe in ethanol–water solution (4:1, v/v, 50 mM HEPES) at pH 6.5, for Ag^+ ion detection [12];

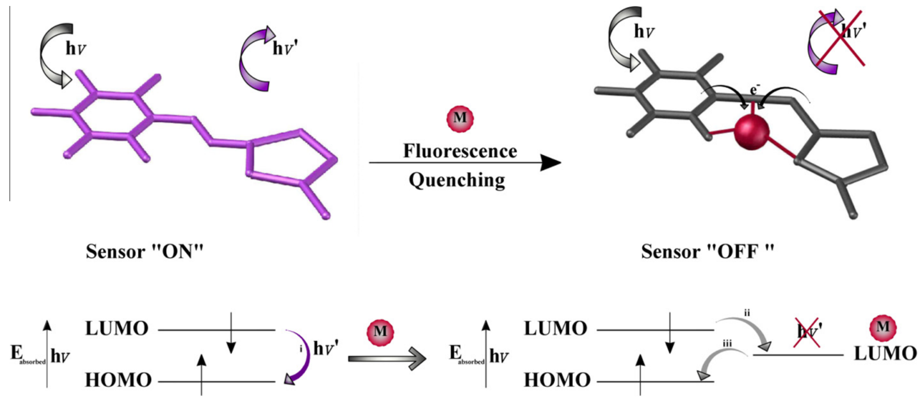

Fig. 4. Orbital energy diagrams for fluorescent "turn-off" PET sensors before and after binding cation and (i) fluorescence emission (ii) forward electron transfer (iii) backward electron transfer processes.

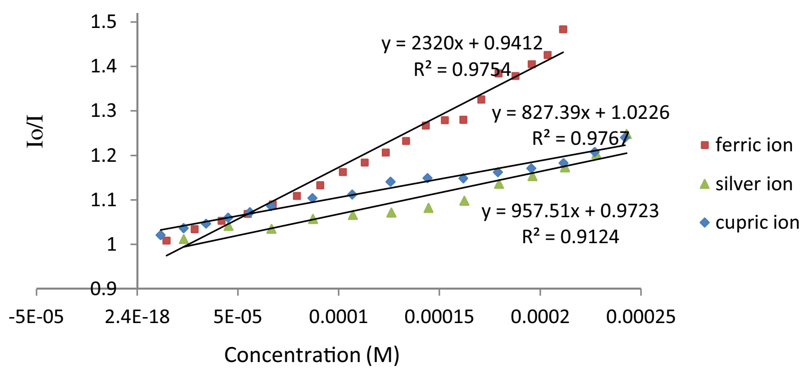

Fig. 5. Stern–Volmer plot for emission intensity quenching of DDUTS in ethanol at various concentrations of ferric, cupric and silver ions. λ_{ex} = 341 nm, λ_{em} = 385 nm.

Table 1
Stern–Volmer constant values for DDUTS in ethanol with Ag^+, Cu^{2+} and Fe^{3+} ions.

Parameter	DDUTS with Ag^+	DDUTS with Cu^{2+}	DDUTS with Fe^{3+}
Ksv (M^{-1})	9.575×10^2	8.273×10^2	23.2×10^2
Regression coefficient (R^2)	0.912	0.976	0.975

2-phenylglycinol functionalized Schiff base in methanol–water (50:50, v/v) [62] and pyrene-based imine chemosensor in water-acetonitrile (30:70, v/v) for Hg^{2+} detection, which exhibited stability for at least 3 days and in the pH range 4.5–12 [63]; ninhydrin–quinoxaline based probe in (ethanol–H_2O, 1:9, v/v) for Cu^{2+} ion sensing [64] and 8-hydroxyquinoline-5-carbaldehyde Schiff-base in 10% (v/v) methanol aqueous medium (acetate buffer, pH 4.5) for Al^{3+} ion detection [65].

Since Schiff bases are generally sensitive towards hydrolysis, numerous research has indicated that this process follows first order kinetics, is accelerated in acidic medium [66,67] and considered very slow in the neutral pH range due to negligible protonation of imine, where the addition of water to the neutral imine is suggested to be the rate-limiting step [68,69]. In this respect, our studies revealed that DDUTS solution in ethanol–water (75:25, v/v) remains stable for a period of 4 days in the dark, after obtaining non-significant variations in absorbance and fluorescence intensities, shapes of the absorption and emission spectra, with no appearance of new bands.

As shown in Fig. 1, DDUTS exhibited strong fluorescent emission at 385 nm upon excitation at 341 nm. The fluorescence emission intensity change of DDUTS in ethanol upon addition of different concentrations of silver, cupric and ferric ions are exhibited in Figs. 1–3, respectively. The fluorescent intensity of probe decreased dramatically upon titration with each of Ag^+, Cu^{2+} and Fe^{3+} ions (fluorescence quenching) and the results showed that the emission intensity was linearly changed with increasing concentration of each ion. The metal ions noticeably perturb the charge distribution of the fluorescent molecule, and its fluorescence is strongly and selectively quenched as a result of the binding event, which constitutes the basis for the determination of Ag^+, Cu^{2+} and Fe^{3+} ions. This fluorescence quenching may occur by excitation energy transfer from the ligand (probe) to the metal d-orbital and/or LMCT [27]. An extremely small amount of sensor, 0.14 μM of probe in this case, was sufficient to detect more than 0.132 μM (14.2 ppb) of Ag^+ ions, 0.088 μM (5.6 ppb) of Cu^{2+} ions and 0.037 μM (2.1 ppb) of Fe^{3+} ions, which make this molecular sensor potentially useful in environmental practice, due to high selectivity and sensitivity.

Stern–Volmer analysis for response of DDUTS in ethanol to Ag^+, Cu^{2+} and Fe^{3+} ions

Emission intensity quenching at various concentrations of silver, cupric and ferric ions have been used to compare the sensing ability of DDUTS towards each ion based on Stern–Volmer analysis. The Stern–Volmer equation:

$$\frac{I_o}{I} = 1 + \mathrm{Ksv}[Q]$$

where I_o is the fluorescence intensity of DDUTS without the corresponding cation, I is the intensity of DDUTS after addition of various concentrations of each cation, Ksv is Stern–Volmer constant and [Q]

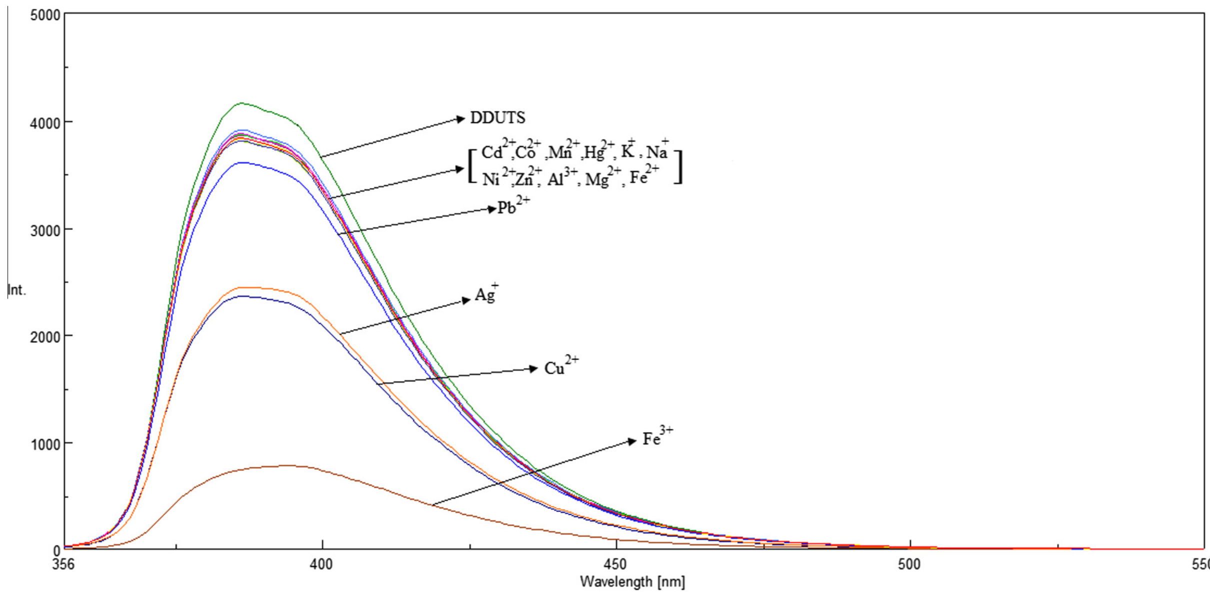

Fig. 6. Fluorescence spectra of DDUTS (0.14 μM) alone and in the presence of several different metal salts (Cd^{2+}, Co^{2+}, Mn^{2+}, Hg^{2+}, K^+, Na^+, Ni^{2+}, Zn^{2+}, Al^{3+}, Mg^{2+}, Fe^{2+}, Pb^{2+}, Ag^+, Cu^{2+} and Fe^{3+} ions: 300 μM) in ethanol. λ_{ex} = 341 nm, λ_{em} = 385 nm.

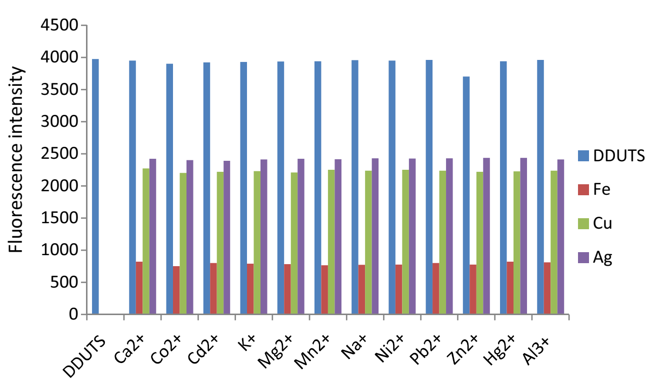

Fig. 7. Competitive selectivity of DDUTS probe (0.14 μM) towards Ag^+, Cu^{2+} and Fe^{3+} ions (300 μM) in the presence of other metal ions: Ca^{2+}, Co^{2+}, Cd^{2+}, K^+, Mg^{2+}, Mn^{2+}, Na^+, Ni^{2+}, Pb^{2+}, Zn^{2+}, $Hg^{2+}$and Al^{3+} ions (300 μM). The first blue bar represents DDUTS alone, the remaining red bars represent solutions containing DDUTS plus Fe^{3+} ions in the absence and in the presence of other competitive metal ions, respectively. Similarly, the green bars represent Cu^{2+} ions and the purple bars represent Ag^+ ions.

is the concentration of the quencher that is ferric, silver or cupric ions. According to Stern–Volmer equation, when all other variables are held constant, the higher the Ksv, the lower the concentration of cation required to quench the emission intensity. The value of Ksv is easily determined from the slope of the plot intensity change versus concentration of each ion. The Stern–Volmer plots for DDUTS in ethanol are shown in Fig. 5. The values of Stern–Volmer constant (Ksv) for DDUTS in ethanol calculated from the slope of the plots for Ag^+, Cu^{2+} and Fe^{3+} ions, are listed in Table 1.

The nature of the Stern–Volmer plots is examined and shows linear dependence of (I_o/I) with Ag^+, Cu^{2+} and Fe^{3+} ion concentrations, with corresponding regression coefficients (R^2) values summarized in Table 1, which indicates the formation of non-fluorescence ground state complex between DDUTS and the quencher i.e., Ag^+, Cu^{2+} and Fe^{3+} ions. The mechanism of quenching and the type of quenching in this case of formation of stable complex between the probe and the cation is photoinduced electron transfer (PET) and static quenching, respectively. The PET process involves the HOMO, LUMO of the fluorophore and the LUMO of the cation after complex formation. In this case, the energy level of the cation LUMO is between the energy levels of the fluorophore HOMO and LUMO, the binding of the cations by the receptor provides a non-radiative path to dissipate the excitation energy, resulting in a quenching of the fluorescence of the chemosensor (Fig. 4).

Selective recognition of Ag^+, Cu^{2+} and Fe^{3+} ions

For an effective sensor, the high selectivity for the target analyte over potentially competitive species is required. The interference

Table 2
Comparison of some chemosensors for Ag^+, Cu^{2+} and Fe^{3+} ions.

Sensors	[sensor] (μM)	Detection limit (μM)	Sensing metals	Binding constant (M^{-1})	Reference
Coumarindithioate derivative	10	0.4	Hg^{2+} and Ag^+ ions	2.5×10^4–5.13×10^4	[11]
2,7-Diferrocenyl-3,6-diazaocta-2,6-diene	50	50	Zn^{2+} and Ag^+ ions	75	[16]
Heptamethine cyanine based	10	0.093	Cu^{2+} ions	6.3×10^4	[17]
Coumarin Schiff base	10	–	Cu^{2+} ions	1.75×10^6	[21]
Coumarin-based	2	51.7–127	Cu^{2+} and Fe^{3+} ions	NA	[26]
Coumarin-derived	5	0.5	Cu^{2+} ions	1.17×10^5	[27]
Rhodamine B hydrazide hydrazone derivative	10	0.0796	Cu^{2+} ions	1.92×10^6	[29]
Carboxylic acid-functionalized tris(2,2′-bipyridine)-ruthenium(II) complex	10	0.042	Cu^{2+} ions	2×10^5	[30]
Thiourea-based	80	0.1	Cu^{2+} and Hg^{2+} ions	–	[31]
Carbazole-based Schiff base	10	9.5	Cu^{2+} ions	6.1×10^4	[32]
Uracil/thiophene Schiff base	0.14	0.037–0.132	Ag^+, Cu^{2+} and Fe^{3+} ions	1.11×10^3–1.29×10^4	This work

Table 3
Regression analysis data and summary of validation parameters for determination of Ag^+, Cu^{2+} and Fe^{3+} ions by the proposed method.

Parameters	Ag^+	Cu^{2+}	Fe^{3+}
λ_{ex}; λ_{em}	341 nm; 385 nm	341 nm; 385 nm	341 nm; 385 nm
Concentration range (μM)	23.1–257.55	11.6–242.14	14.5–203.74
Regression equation	$Y = -2 \times 10^6 X + 3955$	$Y = -3 \times 10^6 X + 4124$	$Y = -6 \times 10^6 X + 4223$
Correlation coefficient (R^2)	0.993	0.993	0.999
LOD (μM)	0.132	0.088	0.037
LOQ (μM)	0.4	0.267	0.114
Intraday Precision (%RSD, $n = 3$)	0.71	0.52	0.34
Interday Precision (%RSD, $n = 3$)	1.02	0.86	0.59

for a number of common ionic species on the fluorescence determination of the cation of interest (Ag^+, Cu^{2+} and Fe^{3+}) was investigated. Competition experiments were carried out by recording the changes of the fluorescence intensity before and after adding the interferants into the probe solution (maintained at 0.14 μM in ethanol, $\lambda_{ex} = 341$ nm, $\lambda_{em} = 385$ nm). Addition of 300 μM of aqueous solution of Ca^{2+}, Co^{2+}, Cd^{2+}, K^+, Mg^{2+}, Mn^{2+}, Na^+, Ni^{2+}, Pb^{2+}, Zn^{2+}, Hg^{2+}, Al^{3+} and Fe^{2+} ions, did not produce significant fluorescence intensity changes. Nevertheless, upon addition of Ag^+, Cu^{2+} and Fe^{3+} ions (300 μM) to the solution containing DDUTS and other metal ion, immediate decreases in fluorescence emission were observed. The fluorescence intensity of probe towards the surveyed metal ions is displayed in Figs. 6 and 7. Therefore, the sensor has a better selectivity for Ag^+, Cu^{2+} and Fe^{3+} over other metal ions tested under the same conditions, the relative error was within ±5%. It was also noticed that the three assayed ions exhibited additive quenching when mixed together.

It is well known that Ag speciation in sea waters is dominated by $AgCl_x^-$ complexes, thus marine organisms have some protection against the toxic Ag^+ ion, as well as hydrophobic organic complexes which cannot form due to intense competition by high Cl^- ion concentrations. Whereas, in fresh waters and as a result of low Cl^- levels, there is more opportunity for Ag^+ to both exist freely or to bind organic ligands or other inorganic anions in freshwater [70]. Complexation of metal ions with organic ligands to create hydrophilic complexes which remain in solution reduces metal toxicity, while complexation to form hydrophobic complexes capable of passive diffusion across cell membranes increases metal toxicity. The free ion model of toxicity states that the proportion of free metals ions available to cells influences toxicity [71], and in freshwater, there is much less opportunity for free Ag^+ to bind

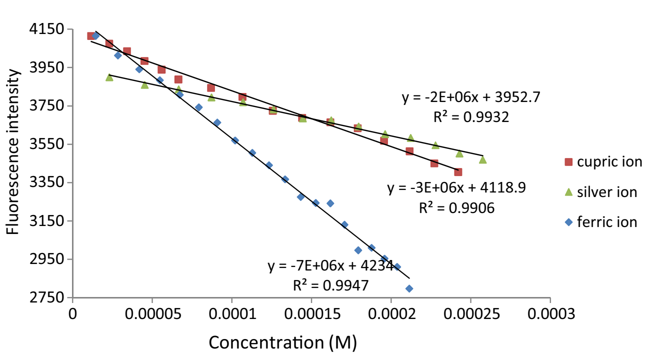

Fig. 8. Calibration Curve plot of cupric, silver and ferric ions based on mean fluorescence intensity of five sets *vs* conc. (M).

with chloride ion to form the low-toxicity $AgCl_x^-$ species [72]. In order to determine the influence of anions on the determination of silver ions, the recovery of 50 μM Ag^+ ions was examined in binary mixtures containing silver ions and one of the tested foreign anions. The following excess of anions, which is expected to be present in sample solutions, did not interfere with the assay (caused a relative error of less than 5%): more than a 10-fold amount of NO_3^-, CH_3COO^-, SO_4^{2-}, PO_4^{3-}, $C_2O_4^{2-}$ and of I^-, F^-, Cl^- and Br^-. This leads to a conclusion that most of the investigated anions do not interfere in determination of silver ions in water samples.

Comparison of DDUTS with common chemosensors

As part of our continuous effort for providing useful analytical methodologies to monitor the increasing number of analytes of environmental relevance as quickly and as cheaply as possible and with the highest sensitivity, this paper describes the synthesis of a new molecular fluorescent probe, *5-amino-1,3-dimethyl-6-(((5-methylthiophen-2-yl)methylene)amino)pyrimidine-2,4(1H,3H)-dione*, which was validated for detection and quantification of Ag^+, Cu^{2+} and Fe^{3+} ions in real samples. The probe has high extinction coefficients, is readily soluble in absolute ethanol and has excitation/emission wavelengths very close to the visible region. The synthesized probe was compared with some reported chemosensors for Ag^+, Cu^{2+} and Fe^{3+} ions (Table 2). While each chemosensor showed some advantages such as high sensitivity, selectivity, naked eye detection and application in living cell imaging, the attractive features of this intensely fluorescent molecule are: easy, practical and cost effective synthesis (one-step reaction with good yield, mild reaction conditions, no need for lengthy synthesis procedures and chromatographic purification), multi-analyte sensing and determination, wide linear response range, reversibility in binding to the analyzed cations; also shows high accuracy and precision, low detection limits, high sensitivities, rapid detection and highest activity at the lowest concentration (0.14 μM probe solution in ethanol).

Method validation in quantitative assay of Ag^+, Cu^{2+} and Fe^{3+} ions

Validation of the method was done according to International Conference on Harmonization (ICH) guidelines.

Linearity

The linearity of the method is its ability to elicit test results that are directly proportional to the concentration of the analyte in the samples. Linearity of the method was evaluated by analyzing different concentrations of working standard solutions of each cation (Ag^+, Cu^{2+} and Fe^{3+}) in the ranges listed in Table 3. Calibration curves were plotted between fluorescence intensity versus concentration of respective working standards (Fig. 8). Each concentration

Table 4
Recovery data of Ag^+, Cu^{2+} and Fe^{3+} ions.

Cation	Taken amount (μM)	Added amount (μM)	Recovered amount (μM)	%Recovery ± SD ($n = 3$)
Fe^{3+}	20	10	29.56	100.95 ± 0.26
		20	40.6	101.52 ± 0.14
		25	44.31	98.00 ± 0.41
Cu^{2+}	40	30	69.22	99.31 ± 0.73
		40	79.05	98.43 ± 0.29
		45	85.89	99.16 ± 0.66
Ag^+	50	40	90.19	100.64 ± 0.34
		50	99.41	101.09 ± 0.85
		55	105.97	101.91 ± 0.40

was repeated three times. The assay was performed according to the experimental conditions previously mentioned (Table 3).

Accuracy

The accuracy of the method was checked by recovery determinations. The determination was done over three concentration levels as blind samples in triplicate according to the ICH guidelines. The concentrations were obtained from the corresponding regression equations then the percentage recoveries were calculated. Accuracy of the method was further assured by the use of the standard addition method, where known amounts of the analyzed cation were added to known concentrations of the sample; the resulting mixtures were assayed, and the results obtained were compared with the expected values, as given in Table 4. The good recoveries of the standard addition technique suggested a good accuracy of the proposed methods.

Precision

Precision of the assay was determined by repeatability (intra-day) and intermediate precision (inter-day). Repeatability refers to the use of the analytical procedure within a laboratory over short period of time that was evaluated by assaying the Quantifiable Concentration (QC) samples during the same day and on different times using new solutions. Intermediate precision was assessed by comparing the assay on different days (3 days), three replicates of each QC sample pool at low (9×10^{-6} M), middle (5×10^{-5} M), and high (2×10^{-4} M) concentrations were assayed according to the ICH requirements. Percentage relative standard deviation (%RSD) was calculated (Table 3).

Detection and quantification limits in analysis of Ag^+, Cu^{2+} and Fe^{3+} ions

The limit of detection (LOD) and the limit of quantification (LOQ) of the cations were derived by calculating the signal-to-noise ratio (S/N) using the following equations designated by ICH guidelines.

$$\mathrm{LOD} = 3.3 \times \sigma / S$$

$$\mathrm{LOQ} = 10 \times \sigma / S$$

where, σ = the standard deviation of the response of the blank and S = slope of the calibration curve. In this respect, a series of blank (samples that do not contain analyte) were tested in ten replicates in ethanol solvent and the mean blank value and standard deviation were calculated. The LOD and LOQ are listed in Table 3. The value is lower than the limit of Ag^+, Cu^{2+} and Fe^{3+} ions in drinking water defined by the U.S. Environmental Protection Agency.

Determination of binding stoichiometry and the association constants Ka of Ag^+, Cu^{2+} and Fe^{3+} ions binding to chemosensor

The method of continuous variation (Job's method) was used to determine the stoichiometry of the complex formed between DDUTS and each of Ag^+, Cu^{2+} and Fe^{3+} ions. The fluorescence intensity at 385 nm was plotted against the molar fraction under a constant total concentration. The tested solution approached a minimal intensity when the molar fraction of cation ([cation]/([cation]+[DDUTS]) was 0.33 (Ag^+ and Cu^{2+}) and 0.66 (Fe^{3+}). These results indicate that chemosensor forms a 2:1 complex with Ag^+ and Cu^{2+} and 1:2 complex with Fe^{3+}. This was also supported by the Benesi–Hildebrand equation [73]:

$$1/(F - F_0) = 1/\{K_a \times (F_{max} - F_0) \times [M^{n+}]^m\} + 1/(F_{max} - F_0)$$

where K_a is the stability constant for complex formation, F_0 is the fluorescence intensity of the probe at the emission λ_{max}(385 nm) in the absence of metal ion. F is the observed fluorescence intensity as a function of the metal concentration ($[M^{n+}]$: Ag^+, Cu^{2+} or Fe^{3+} ions) and F_{max} is the maximal fluorescence intensity in the presence of an excess of these ions in solution (600 μM). It is well known that m is equal to 0.5 for 2:1 complexation; m is equal to 1 for 1:1 complexation, and m = 2 for 1:2 complexation, etc. Analysis of the emission titration curves by the Benesi–Hildebrand plots (Fig. 9A–C) shows the formation of 2:1 complex between the sensor and Ag^+ or Cu^{2+} ions (m = 0.5); and a 1:2 stoichiometry exists with Fe^{3+} ions. These results are in good accordance with the values obtained from the Job's method. The binding constant K_a (M^{-1}) is determined from the ratio of intercept and slope of Benesi–Hildebrand plot of emission intensities. The free energy changes ΔG (kJ/mol) for the

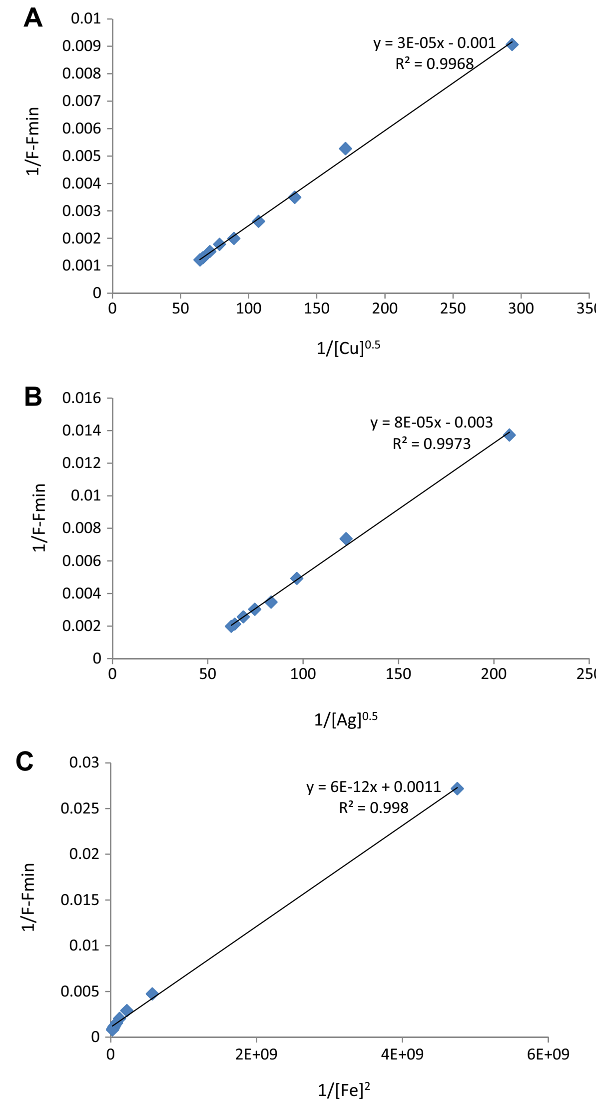

Fig. 9. (A) Benesi–Hildebrand plot of probe assuming 2:1 binding stoichiometry with Cu^{2+}. (B) Benesi–Hildebrand plot of probe assuming 2:1 binding stoichiometry with Ag^+. (C) Benesi–Hildebrand plot of probe 1:2 binding stoichiometry with Fe^{3+}.

Table 5
Calculated thermodynamic parameters for Ag^+, Cu^{2+} and Fe^{3+} ions.

Metal ions	Ka (M^{-1})	$-\Delta G$ (kJ/mole)
Ag^+	1.4062×10^3	17.96
Cu^{2+}	1.1111×10^3	17.38
Fe^{3+}	1.2909×10^4	23.45

Table 6
Recovery study of spiked determination of Ag^{+}, Cu^{2+} and Fe^{3+} ions in water sample with proposed probe.

Sample	Ag^{+}			Cu^{2+}			Fe^{3+}		
	Spiked amount (μM)	Recovered amount (μM)	%Recovery ± SD (n = 3)	Spiked amount (μM)	Recovered amount (μM)	%Recovery ± SD (n = 3)	Spiked amount (μM)	Recovered amount (μM)	%Recovery ± SD (n = 3)
1	0	0	–	0	0	–	0	0	–
2	50	50.67	98.56 ± 0.24	30	31.25	98.87 ± 0.13	40	38.02	98.54 ± 0.33
3	250	249.13	99.43 ± 0.14	150	148.36	100.65 ± 0.38	200	200.37	101.4 ± 0.39

chemosensor–metal ions complexation was determined using the relation $\Delta G = -RT \ln K$ (Table 5).

Study on reversibility and mechanism for the binding of DDUTS with Ag^{+}, Cu^{2+} and Fe^{3+} ions

It is well known that the reversibility is an important property to obtain an excellent probe. Thus, EDTA titrations were conducted to examine the reversibility of the probe. The fluorescence intensity increased when $EDTANa_2$ (as chelating agent) was added to the solution containing probe (0.14 μM) and Ag^{+} (100 μM), Cu^{2+} (100 μM) or Fe^{3+} (100 μM). When Ag^{+}, $Cu^{2+}$and Fe^{3+} ions were added to the system again, the signals were almost completely reproduced. These findings indicated that probe can reversibly coordinate with Ag^{+}, Cu^{2+} and Fe^{3+} ions. These results reveal that the binding of probe and analyzed cations is reversible rather than a cation-catalyzed reaction.

Effect of standing time on complexation

Ag^{+}, Cu^{2+} and Fe^{3+} ions immediately form complexes with DDUTS probe. The emission intensities of these complexes remained constant for up to 2 h.

Preliminary analytical application

The water resource may be contaminated by Ag^{+}, Cu^{2+} and Fe^{3+} ions from the industrial waste. Generally, one of the most important and useful applications for a fluorescent probe is the detection of metal ions in water samples. Thus, the proposed methods was applied to the determination of Ag^{+}, Cu^{2+} and Fe^{3+} ions in tap water samples from Debbieh–Lebanon, and were filtered before use. For determination of silver in fresh water, 5 mL sample was transferred into a 100 mL volumetric flask and diluted with distilled water. The pH of the solution was adjusted to 5 by using 0.1 M solution of HNO_3. In this condition, the silver is in the form of Ag^{+} and the pH of the solution is in the working pH range of the sensor.

After the probe being treated with the water samples, fluorescence intensity of probe was determined. It was found that silver, cupric and ferric ions were not detected in the water samples. Next the water samples were spiked with each cation standard solutions at different concentration levels, and then analyzed their concentrations with proposed method. Results are shown in Table 6. One can notice that the recovery study of spiked samples determined by the probe showed satisfactory results. Thus, the present probe is useful for the determination of Ag^{+}, Cu^{2+} and Fe^{3+} ions in real samples.

Conclusion

The present work describes a new diaminouracil-thiophene aldehyde Schiff base derivative as a fluorescent chemosensor for both recognition and quantification of Ag^{+}, Cu^{2+} and Fe^{3+} ions. The probe can be easily synthesized in a one-step reaction, and exhibited high selectivity and sensitivity to Ag^{+}, Cu^{2+} and Fe^{3+} ions in ethanol through remarkable quenching effect of these cations on the probe's fluorescence intensity. The quenching process is reversible and is hardly affected by other coexisting metal ions. The proposed method has the advantage over other published methods of detecting ternary cation mixture and could be applied for the determination of Ag^{+}, Cu^{2+} and Fe^{3+} ions in environmental water testing due to its excellent accuracy, precision and sensitivity.

Acknowledgements

Dr K. Bouhadir is grateful to the Lebanese National Council for Scientific Research (LNCSR) and the University Research Board (URB) at the American University of Beirut (AUB).

References

[1] S. Khan, Q. Cao, Y.M. Zheng, Y.Z. Huang, Y.G. Zhu, Environ. Pollut. 152 (2008) 686–692.
[2] W.Y. Lim, A.Z. Aris, M.P. Zakaria, Sci. World J. 2012 (2012) 1–14.
[3] M. Harmanescu, L.M. Alda, D.M. Bordean, I. Gogoasa, I. Gergen, Chem. Cent. J. 5 (2011) 1–10.
[4] N.L. Ibrahim, Anat. Physiol. 4 (2013) 1–34.
[5] S. Asghari, S.A. Johari, J.H. Lee, Y.S. Kim, Y.B. Jeon, H.J. Choi, M.C. Moon, I.J. Yu, J. Nanobiotechnol. 10 (2012) 1–11.
[6] P.V. AshaRani, G.L.K. Mun, M.P. Hande, S. Valiyaveettil, ACS Nano 3 (2009) 279–290.
[7] United States Environmental Protection Agency, National Primary Drinking Water Regulations MCL booklet, EPA 816-F-09-004 (2009). <http://water.epa.gov/drink/contaminants/upload/mcl.pdf>.
[8] I. Leray, B. Valeur, Eur. J. Inorg. Chem. 24 (2009) 3525–3535.
[9] Y. Hongyao, Z. Xiaoying, X. Haibo, J. Shanghai Normal Univ. (Nat. Sci.) 41 (2012) 638–645.
[10] W. Pu, H. Zhao, C. Huang, L. Wu, D. Xua, Microchim. Acta 177 (2012) 137–144.
[11] H.A. El-Shekheby, A.H. Mangood, S.M. Hamza, A.S. Al-Kady, El-Z.M. Ebeid, Luminescence 29 (2014) 158–167.
[12] C. Yu, J. Zhang, M. Ding, L. Chen, Anal. Methods 4 (2012) 342–344.
[13] Y. Wen, F. Xing, S. He, S. Song, L. Wang, Y. Long, D. Li, C. Fan, Chem. Commun. 46 (2010) 2596–2598.
[14] I. Takashima, A. Kanegae, M. Sugimoto, A. Ojida, Inorg. Chem. 53 (2014) 7080–7082.
[15] C. Huang, A. Ren, C. Feng, N. Yang, Sens. Actuators B Chem. 151 (2010) 236–242.
[16] K. Dutta, D.K. Das, Indian J. Chem. 51A (2012) 816–820.
[17] Z. Han, Q. Yang, L. Liang, X. Zhang, Adv. Mater. Phys. Chem. 3 (2013) 314–319.
[18] M. Zhou, J. Huang, Z. Liu, W. Zeng, J. Nucl. Med. 53 (2012) 1593–1600.
[19] X. Xu-zhi, C. Peng, C. He-ru, Chem. Res. Chin. Univ. 28 (2012) 609–613.
[20] M.T. Morgan, P. Bagchi, C.J. Fahrni, Dalton Trans. 42 (2013) 3240–3248.
[21] Y.W. Duan, H.Y. Tang, Y. Guo, Z.K. Song, M.J. Peng, Y. Yan, Chin. Chem. Lett. 25 (2014) 1082–1086.
[22] P. Li, X. Duan, Z. Chen, Y. Liu, T. Xie, L. Fang, X. Li, M. Yin, B. Tang, Chem. Commun. (Camb.) 47 (2011) 7755–7757.
[23] K. Mahiya, P. Mathur, J. Fluoresc. 23 (2013) 767–776.
[24] M. Zhang, H.N. Le, X.Q. Jiang, S.M. Guo, H.J. Yu, B.C. Ye, Talanta 117 (2013) 399–404.
[25] D. Udhayakumari, S. Velmathi, Y.M. Sung, S.P. Wu, Sens. Actuators B Chem. 198 (2014) 285–293.
[26] O. García-Beltrán, B.K. Cassels, C. Pérez, N. Mena, M.T. Núñez, N.P. Martínez, P. Pavez, M.E. Aliaga, Sensors 14 (2014) 1358–1371.
[27] H.S. Jung, P.S. Kwon, J.W. Lee, J.I. Kim, C.S. Hong, J.W. Kim, S. Yan, J.Y. Lee, J.H. Lee, T. Joo, J.S. Kim, J. Am. Chem. Soc. 131 (2009) 2008–2012.
[28] Y.C. Wang, L.Z. Liu, Y.M. Pan, H.S. Wang, Molecules 16 (2011) 100–106.
[29] L. Tang, J. Guo, N. Wang, Bull. Korean Chem. Soc. 34 (2013) 159–163.
[30] C.L. He, F.L. Ren, X.B. Zhang, Y.Y. Dong, Y. Zhao, Anal. Sci. 22 (2006) 1547–1551.
[31] P. Qin, C. Niu, G. Zeng, J. Zhu, L. Yue, Anal. Sci. 24 (2008) 1205–1208.
[32] L. Tang, D. Wu, S. Hou, X. Wen, X. Dai, Bull. Korean Chem. Soc. 35 (2014) 2326–2329.

[33] C. Yu, J. Zhang, R. Wang, L. Chen, Org. Biomol. Chem. 8 (2010) 5277–5279.
[34] G.Y. Lan, C.C. Huang, H.T. Chang, Chem. Commun. (Camb.) 46 (2010) 1257–1259.
[35] S. Goswami, D. Sen, N.K. Das, Org. Lett. 12 (2010) 856–859.
[36] T. Moriuchi-Kawakami, Y. Hisada, Y. Shibutani, Chem. Cent. J. 4 (2010) 1–6.
[37] W. Sun, Y. Du, Y. Wang, J. Lumin. 130 (2010) 1463–1469.
[38] N.R. Chereddy, M.V.N. Raju, P. Nagaraju, V.R. Krishnaswamy, P.S. Korrapati, P.R. Bangal, V.J. Rao, Analyst 139 (2014) 6352–6356.
[39] M. Zheng, H. Tan, Z. Xie, L. Zhang, X. Jing, Z. Sun, Appl. Mater. Interfaces 5 (2013) 1078–1083.
[40] M.F. Yoder, W.S. Kisaalita, J. Biol. Eng. 5 (2011) 1–12.
[41] L. Zhou, H. Zhang, Y. Luan, S. Cheng, L.J. Fan, Nano-Micro Lett. 6 (2014) 327–334.
[42] Y. Wei-Guo, C. Zhong, Y. Dong, C. Ting-Ting, X. Lin, Chin. J. Anal. Chem. 40 (2012) 1241–1246.
[43] M.J.C. Marenco, C. Fowley, B.W. Hyland, G.R.C. Hamilton, D. Galindo-Riaño, J.F. Callan, Tetrahedron Lett. 53 (2012) 670–673.
[44] Y.M. Ma, R.C. Hider, Bioorg. Med. Chem. 1 (2009) 8093–8101.
[45] H. Wang, D. Wang, Q. Wang, X. Li, C.A. Schalley, Org. Biomol. Chem. 8 (2010) 1017–1026.
[46] F. Thomas, G. Serratrice, C. Béguin, E.S. Aman, J.L. Pierre, F. Marc, J.P. Laulhére, J. Biol. Chem. 274 (1999) 13375–13383.
[47] J. Mao, Q. He, W. Liu, Talanta 80 (2010) 2093–2098.
[48] L. Long, L. Zhou, L. Wang, S. Meng, A. Gong, C. Zhang, Anal. Chim. Acta 812 (2014) 145–151.
[49] S. Wang, X. Meng, M. Zhu, Tetrahedron Lett. 52 (2011) 2840–2843.
[50] L. Zhang, J. Wang, J. Fan, K. Guo, X. Peng, Bioorg. Med. Chem. Lett. 21 (2011) 5413–5416.
[51] I. Moczar, P. Huszthy, A. Mezei, M. Kadar, J. Nyitrai, Tetrahedron 66 (2010) 350–358.
[52] B. Bodenant, T. Weil, M. Businelli-Pourcel, F. Fages, B. Barbe, I. Pianet, M. Laguerre, J. Org. Chem. 64 (1999) 7034–7039.
[53] R. Joseph, B. Ramanujam, H. Pal, C.P. Rao, Tetrahedron Lett. 49 (2008) 6257–6261.
[54] F. Unob, Z. Asfari, J. Vicens, Tetrahedron Lett. 39 (1998) 2951–2954.
[55] Y.D. Cao, Q.Y. Zheng, C.F. Chen, Z.T. Huang, Tetrahedron Lett. 44 (2003) 4751–4755.
[56] L. Wang, W. Qin, X. Tang, W. Dou, W. Liu, J. Phys. Chem. A 115 (2011) 1609–1616.
[57] T. Lou, Z. Chen, Y. Wang, L. Chen, Appl. Mater. Interfaces 3 (2011) 1568–1573.
[58] S. Devaraj, M. Kandaswamy, Opt. Photonics J. 3 (2013) 32–39.
[59] S.K. Kim, S.H. Lee, J.Y. Lee, J.Y. Lee, R.A. Bartsch, J.S. Kim, J. Am. Chem. Soc. 126 (2004) 16499–16506.
[60] J.S. Kim, H.J. Kim, H.M. Kim, S.H. Kim, J.W. Lee, S.K. Kim, B.R. Cho, J. Org. Chem. 71 (2006) 8016–8022.
[61] J.Y. Noh, I.H. Hwang, H. Kim, E.J. Song, K.B. Kim, C. Kim, Bull. Korean Chem. Soc. 34 (2013) 1985–1989.
[62] A. Jiménez-Sánchez, N. Farfán, R. Santillan, Tetrahedron Lett. 54 (2013) 5279–5283.
[63] G. Sivaraman, T. Anand, D. Chellappa, RSC Adv. 2 (2012) 10605–10609.
[64] A. Kumar, V. Kumar, U. Diwan, K.K. Upadhyay, Sens. Actuators B Chem. 176 (2013) 420–427.
[65] X. Jiang, B. Wang, Z. Yang, Y. Liu, T. Li, Z. Liu, Inorg. Chem. Commun. 14 (2011) 1224–1227.
[66] F. Benachenhou, N. Mimouni, Y. Mederbel, R.K. Slimane, Arabian J. Chem. 5 (2012) 245–250.
[67] H. Hassib, N.S. Abdel-Kader, Y. Issa, J. Solution Chem. 41 (2012) 2036–2046.
[68] A.S. Kirdant, B.K. Magar, T.K. Chondhekar, Der Chemica Sinica 3 (2012) 52–58.
[69] L. Matesic, J.M. Locke, K.L. Vine, M. Ranson, J.B. Bremner, D. Skropeta, Bioorg. Med. Chem. 19 (2011) 1771–1778.
[70] F. Valverde, M. Costas, F. Pena, I. Lavilla, C. Bendicho, Chem. Speciat. Bioavailab. 20 (2008) 217–226.
[71] J.T. Phinney, K.W. Bruland, Environ. Toxicol. Chem. 16 (1997) 2046–2053.
[72] H.T. Ratte, Environ. Toxicol. Chem. 18 (1999) 89–108.
[73] S. Dalapati, B.K. Paul, S. Jana, N. Guchhait, Sens. Actuators B Chem. 157 (2011) 615–620.